Acta Biologica Szegediensis

Volume 69(1):38-43, 2025
Acta Biologica Szegediensis
http://abs.bibl.u-szeged.hu/index.php/abs
DOI:10.14232/abs.2025.1.38-43

ARTICLE

The pathogenesis-related protein 1 (*PR-1*) gene in rice (*Oryza sativa*): isolation, sequencing and bioinformatics analysis

Fadime Beyazyuz[1] and Ertugrul Filiz[2,*]

[1]Department of Forest Engineering, Faculty of Forestry, Duzce University, Duzce, Türkiye
[2]Department of Crop and Animal Production, Cilimli Vocational School, Duzce University, Cilimli, Duzce, Türkiye

ABSTRACT Pathogenesis-related 1 (PR1) proteins constitute an important gene family that participates in plant responses to both biotic and abiotic stresses. The aim of this study was to isolate and sequence a PR1 gene from rice (*Oryza sativa*) and to characterize the encoded protein using bioinformatics tools. Sequencing revealed a 441-bp exon encoding a 147-amino-acid protein. OsPR1 contained a PF00188 cysteine-rich secretory protein (CAP) domain and a 21-amino-acid signal peptide. Phylogenetic analysis indicated that OsPR1 is clustered with PR1 proteins from *Sorghum bicolor* and *Zea mays* within the monocot clade. Protein–protein interaction predictions suggested putative functional associations of OsPR1 with enzymes involved in nitrogen and purine metabolism. Structural modeling and comparison with *Arabidopsis thaliana* PR1 (AtPR1) revealed a high degree of three-dimensional conservation. These data provide experimental confirmation of a rice PR1 gene and offer a framework for future functional studies on PR1-mediated stress responses in rice.
Acta Biol Szeged 69(1):38-43 (2025)

KEY WORDS
bioinformatics
DNA sequencing
Oryza sativa
pathogenesis-related protein 1
phylogeny
protein modeling

ARTICLE INFORMATION
Submitted
08 July 2025
Accepted
18 November 2025
***Corresponding author**
E-mail: ertugrulfiliz@gmail.com

Introduction

Plants have evolved sophisticated mechanisms to protect themselves against pathogens and pests. Pathogenesis-related (PR) proteins are key components of these defense responses and are classified into at least 17 families based on sequence similarity, structural features and enzymatic activities (van Loon et al. 2006). PR1 proteins were first described in tobacco leaves infected with tobacco mosaic virus and can account for up to 2% of total soluble protein in infected tissue (Alexander et al. 1993). PR1 proteins can be either acidic or basic and are usually secreted into the apoplast, although vacuolar localization has also been reported (Sessa et al. 1995).

All PR1 proteins share a conserved CAP (cysteine-rich secretory protein, antigen 5, pathogenesis-related 1) domain of approximately 150 amino acids. This domain comprises four α-helices and four β-strands stabilized by disulfide bonds and contains a caveolin-binding motif (CBM) implicated in sterol binding and antimicrobial activity (Breen et al. 2017). Besides their established roles in pathogen defense, functional annotation and expression analyses have linked PR1 genes to broader stress tolerance mechanisms in plants (Zaynab et al. 2021).

Genome-wide surveys have identified PR1 gene families in several species, including soybean (Almeida-Silva and Venancio 2022), *Musa* spp. (Anuradha et al. 2022), *Piper nigrum* (Kattupalli et al. 2021), barley (Yin et al. 2023), tomato (*Solanum lycopersicum*) (Akbudak et al. 2020) and potato (*Solanum tuberosum*) (Zaynab et al. 2021). In *Oryza sativa*, Liu and Xue (2006) computationally identified 23 PR1-type candidate genes, the majority of which had not been experimentally characterized.

Despite this in silico catalog, there is limited experimental information on individual rice PR1 genes and their structural and functional properties. In the present study, we amplified and sequenced an *O. sativa* PR1 gene (OsPR1) and performed an in-depth bioinformatic analysis, including domain architecture, post-translational modification predictions, phylogenetic relationships, protein–protein interaction (PPI) networks and three-dimensional (3D) structural modeling.

Materials and methods

Plant material and DNA isolation

Seeds of the rice cultivar *Oryza sativa* var. Osmancık were obtained from Duzce, Türkiye. Seeds were surface sterilized with 70% ethanol for 1 min followed by 2% sodium hypochlorite for 10 min and rinsed three times with sterile distilled water. Sterilized seeds were germinated in vitro on MS basal medium (Murashige and Skoog,

1962) under aseptic conditions. Germination was carried out at 25 °C, under a 16 h light/8 h dark photoperiod for approximately 7 days. After the emergence of seedlings, plants were transferred to hydroponic MS medium and maintained for an additional 7 days to promote early vegetative development. Subsequently, 14-day-old seedlings were transplanted to pots containing a peat:perlite mixture (3:1) and grown in a controlled greenhouse at 25 °C, 50% relative humidity, and long-day (16 h light/8 h dark) conditions (light intensity: 140 μmol m^{-2} s^{-1}). Plants were irrigated with tap water at three-day intervals. Leaves were harvested 30 days after sowing for genomic DNA isolation, OsPR1 amplification and sequencing. Genomic DNA was extracted from leaves using the DNA Plant Mini Kit (E.Z.N.A., Cat. No: 2485-01) following the manufacturer's protocol. DNA quality was examined by agarose gel electrophoresis and concentrations were determined using a NanoDrop spectrophotometer (Biospec Nano, Shimadzu, Japan).

Primer design and PCR amplification

Degenerate primers for amplifying OsPR1 were designed based on the *Arabidopsis thaliana* PR1 protein sequence (UniProt Q9ZNS4, locus At2g14580) using the Primer3 server (https://primer3.ut.ee/) and sequence information retrieved from UniProt (https://www.uniprot.org/). The amplified 441-bp fragment was analyzed by BLASTn and showed 100% identity to the *O. sativa* PR1 locus (GenBank accession PQ582227), corresponding to the exon region of gene model Os07g0129200. The confirmed OsPR1 nucleotide sequence is provided as Supplementary Data (FASTA format). The primer sequences were:

Forward: 5′-ATC ATCTCTTCGTCTACTAA-3′
Reverse: 5′-GCAAATACGGCTGACAGTAC-3′

PCR reactions (50 μL) were prepared using GoTaq® Green Master Mix (2×) (Promega, USA) with the following final composition: 25 μL of 2× GoTaq Master Mix, 2 μL template DNA, 1 μL of each primer (10 pmol), and 21 μL nuclease-free water to reach a final volume of 50 μL. The thermal cycling conditions were as follows: 94 °C for 5 min, followed by 40 cycles of 94 °C for 30 s, 51 °C for 30 s, and 72 °C for 1 min, with a final extension at 72 °C for 7 min. PCR products were separated on 1.5% agarose gels to verify the expected amplicon sizes..

Gel extraction and sequencing

PCR products were purified from agarose gels using the Monarch DNA Gel Extraction Kit (New England Biolabs) following the manufacturer's instructions. Purified fragments were sequenced by Macrogen Europe BV (https://www.macrogen-europe.com/).

Bioinformatic analyses

Sequence analyses

The OsPR1 open reading frame (ORF) was translated into an amino acid sequence using the ExPASy Translate tool (https://web.expasy.org/translate/). Basic physicochemical parameters, including molecular weight, theoretical isoelectric point (pI), and the number of charged residues, were calculated using ProtParam (https://web.expasy.org/protparam/) (Gasteiger et al. 2005).

Protein domain architecture was examined using the NCBI Conserved Domain Database (CDD; https://www.ncbi.nlm.nih.gov/Structure/cdd/wrpsb.cgi) (Wang et al. 2023) and the SMART server (http://smart.embl-heidelberg.de/) (Letunic et al. 2021). Putative phosphorylation sites were predicted with NetPhos 3.1 (https://services.healthtech.dtu.dk/services/NetPhos-3.1/). Putative interaction partners of OsPR1 were inferred using STRING v11.0 (https://string-db.org/) (Szklarczyk et al. 2023).

Phylogenetic analyses

Full-length PR1 protein sequences from *O. sativa*, *A. thaliana*, *Glycine max*, *Populus trichocarpa*, *S. lycopersicum*, *Zea mays*, *Brachypodium distachyon*, *Sorghum bicolor* and *Hordeum vulgare* were aligned using BioEdit with default parameters. Poorly aligned positions and sites containing more than 5% gaps were removed using MEGA12's built-in alignment trimming tool. The final trimmed alignment was used to construct a phylogenetic tree in MEGA12 (Kumar et al. 2024) employing the maximum likelihood (ML) method under the LG amino acid substitution model. Branch support was evaluated with 1000 bootstrap replicates.

Predicted secondary and 3D structure analyses

Secondary structure composition (helix, strand and coil content) and Ramachandran plots were obtained using VADAR server v1.8 (http://vadar.wishartlab.com/) (Willard 2003). The 3D structure of OsPR1 was predicted with RoseTTAFold via the Robetta server (https://robetta.bakerlab.org/submit.php) (Baek et al. 2021). For comparative analysis, the PR1 protein from *A. thaliana* (AtPR1; 161 amino acids, accession P33154) was retrieved from UniProt.

Structural similarity between OsPR1 and AtPR1 was quantified using CLICK (https://mspc.bii.a-star.edu.sg/minhn/DNA_protein.html), which computes structure overlap, root mean square deviation (RMSD) and topology scores (Nguyen et al. 2011).

Different complementary tools were employed to predict subcellular localization. Signal peptide presence was analyzed with SignalP 6.0 and was predicted as a

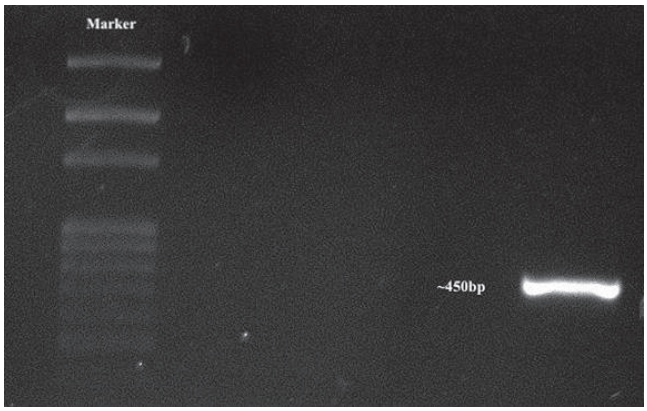

Figure 1. The amplification of OsPR1 from genomic DNA of *O. sativa*. The expected 441-bp band is indicated by an arrow. Marker specifies the 1.5 kb DNA marker (ABM).

high-confidence N-terminal signal peptide indicating secretion. TargetP 2.0 also identified OsPR1 as a secreted protein with no plastidial or mitochondrial targeting peptides. Moreover, WoLF PSORT predicted an extracellular/apoplastic localization with the highest score among all compartments. Taken together, these results support a predominantly secretory/apoplastic localization, consistent with the general behavior of canonical PR1 proteins in plants.

Results and discussion

OsPR1 isolation and sequence analysis

Genomic DNA was successfully extracted from leaves of *O. sativa* var. Osmancık using the DNA Plant Mini Kit, and high-quality DNA was confirmed by agarose gel electrophoresis. PCR amplification of the OsPR1 locus using the designed primers yielded the expected 441-bp fragment (Fig. 1). BLASTn analysis showed that this fragment was identical to the *O. sativa* PR1 locus (PQ582227), corresponding to the exon region of Os07g0129200.

The OsPR1 ORF encodes a 147-amino-acid protein with a predicted molecular weight of 13.94 kDa and a slightly acidic theoretical pI of 6.03. OsPR1 contains 11 negatively charged residues (Asp + Glu) and 10 positively charged residues (Arg + Lys). In tomato, the *SlPR1* gene (Gen ID: Solyc01g106620.2) encodes a 179-amino-acid PR1 protein from a 540-bp ORF (Chen et al. 2023), indicating moderate length variation among PR1 family members in different species.

Domain analysis using CDD indicated that OsPR1 contains a CAP (CSP/antigen 5/PR1) domain (Fig. 2A). SMART analysis further identified PF00188 (cysteine-rich secretory protein family) and SM000198 (SCP/Tpx-1/Ag5/PR-1/Sc7 family) domains (Fig. 2B), consistent with typical PR1 proteins. A conserved PF00188-associated motif, "VDPHNAGRADVGVGPVSWNDTVAAYAESYAGRRG-GDCALEHSDSGGKYGENIFWGSGGGGWAGGGA-GLGVGVG", was detected using the Pfam database, supporting classification of OsPR1 as a cysteine-rich

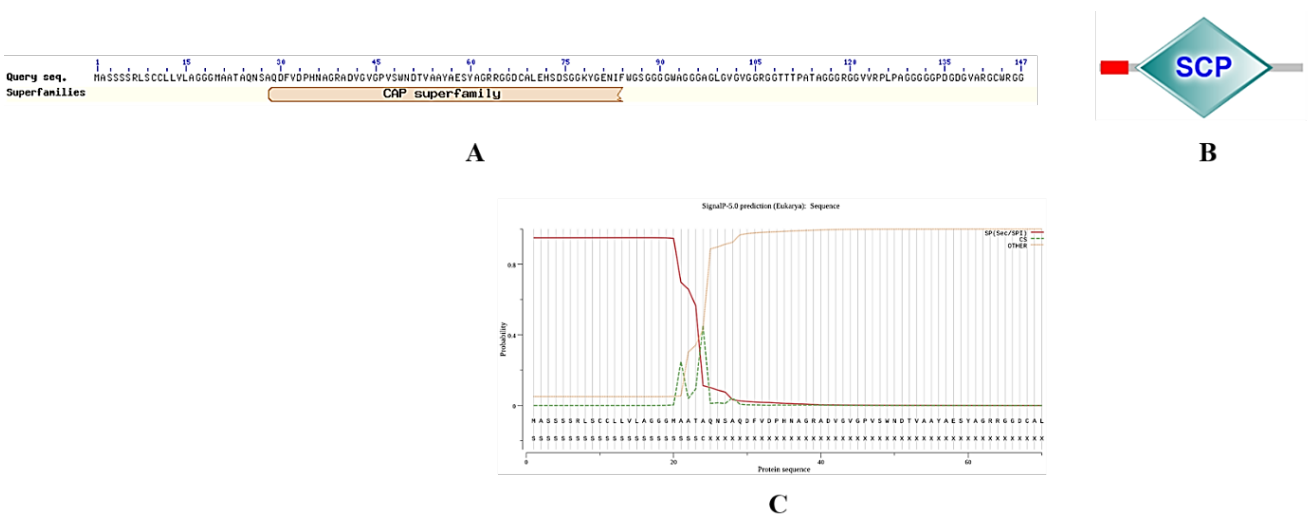

Figure 2. Conserved domain analysis of OsPR1 protein using NCBI Conserved Domain Search (A) and SMART server (B), respectively, including PF00188 (Cysteine-rich secretory protein family) and SM000198 (SCP / Tpx-1 / Ag5 / PR-1 / Sc7 family of extracellular domains) domain structures. In addition, the signal peptide is shown in red in C, and it also showed that residues 1–21 correspond to the signal peptide, and residues 22–147 form the PF00188 CAP domain.

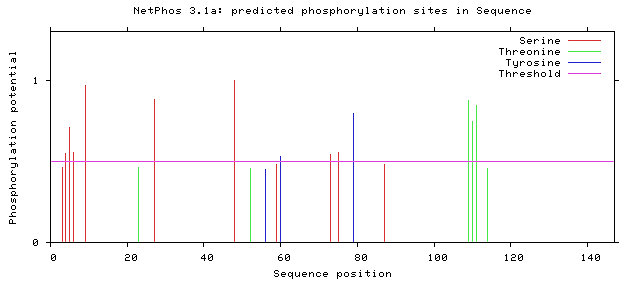

Figure 3 The NetPhos-3.1 server was used to indicate the phosphorylating sites at serine, threonine, and tyrosine on OsPR1 proteins. Serine, threonine and tyrosine are colored red, green and blue, respectively. Additionally, the purple line shows the threshold.

secretory protein.

Signal eptide prediction identified a 21-amino-acid N-terminal signal peptide (residues 1–21), followed by a 126-amino-acid CAP domain (residues 22–147) (Fig. 2C). This organization suggests that OsPR1 is a secreted protein, in line with the extracellular or apoplastic localization reported for other PR1 proteins (Breen et al. 2017; Akbudak et al. 2020).

Phosphorylation site analysis predicted eight serine, three threonine and two tyrosine phosphorylation sites (Fig. 3). Protein phosphorylation on Ser, Thr, and Tyr residues is one of the most common post-translational modifications in plant signaling (Yao et al. 2015). The presence of multiple predicted phosphorylation sites suggests that OsPR1 may be subject to dynamic regulation by kinases in response to environmental or developmental cues.

Phylogenetic analyses

A phylogenetic tree was constructed using full-length PR1 protein sequences from nine plant species (Fig. 4). The resulting topology separated the PR1 proteins into two major clades: Group A (dicots) and Group B (monocots), consistent with monocot–dicot divergence. Within the monocot cluster (Group B), OsPR1 grouped most closely with PR1 homologs from *Zea mays* (ZmPR1; accession Zm00001d019364P001), *Sorghum bicolor* (SbPR1; Sobic.002G105300.1.p) *Brachypodium distachyon* (BdPR1; Brdisv1Bd21-3r1009218m.p) and *Hordeum vulgare* (HORVU.MOREX.r3.5HG0519270.1).These proteins formed a distinct subclade, suggesting conserved sequence features among grass PR1 proteins.

Bootstrap support for the monocot group (51%) was lower than for the dicot group (98%), indicating greater sequence divergence among monocot PR1 proteins. This pattern suggests lineage-specific diversification of PR1 genes in monocot species, possibly reflecting adaptation to distinct pathogen spectra or environmental conditions.

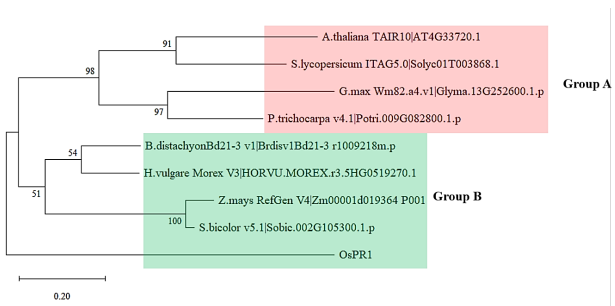

Figure 4. The phylogenetic distribution of PR1 protein sequences from different plant species. A total of nine species were included in the tree, constructed using the ML method with 1000 bootstrap replicates in MEGA12: *O. sativa*, *A. thaliana*, *G. max*, *P. trichocarpa*, *S. lycopersicum*, *Z. mays*, *B. distachyon*, *S. bicolor* and *H. vulgare*.

Interaction networks analysis

Protein–protein interaction networks are central to the coordination of plant development and stress responses and provide insight into functional protein associations (Cuadrado and Van Damme 2024). STRING analysis identified two main clusters and seven putative functional partners for OsPR1 (A0A0N7KMW0) (Fig. 5). These predicted partners included nitrate reductases (NIA1, Q6ZC33 and Q6ZHH7), phosphoribosylamine-glycine ligase (Q2QWF3), phosphoribosylglycinamide synthetase (Q6YZX5), phosphoribosylformylglycinamidine cycloligase (Q850Z8) and a FAD-dependent oxidoreductase, glycerol-3-phosphate dehydrogenase (Q5VQP1).

The PPI network contained 8 nodes and 16 edges, with an average node degree, average local clustering coefficient, and PPI enrichment p-value of 4, 0.93, and 0.124, respectively. Functional enrichment analysis of the PPI network indicated overrepresentation of terms related to

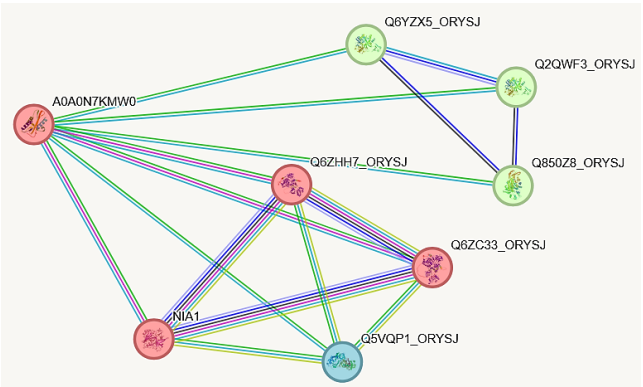

Figure 5. Protein-protein interaction analyses of OsPR1 protein (A0A0N7KMW0) using k-means clustering. The red coloration indicates proteins involved in nitric oxide biosynthesis, while the green coloration signifies proteins associated with purine nucleobase biosynthesis.

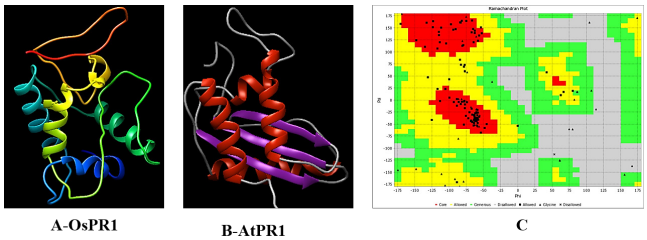

Figure 6. The predicted three-dimensional structure of OsPR-1 and A. thaliana PR1 proteins was generated by RoseTTAFold server (A) and by AlphaFold (B), respectively. Furthermore, the Ramachandran plot of the OsPR1 3D protein structure is displayed in figure C.

nitric oxide biosynthetic process (GO:0006809) and purine nucleobase biosynthetic process (GO:0009113). Molecular function terms included nitrate reductase (NADPH) activity (GO:0050464), nitrate reductase (NADH) activity (GO:0009703) and phosphoribosylamine-glycine ligase activity (GO:0004637). KEGG pathway analysis highlighted nitrogen metabolism (map00910) and purine metabolism (map00230).

Nitrogen (N) is a major determinant of plant growth and yield and plays an important role in stress resistance and host–pathogen interactions. Nitrogen supply, N-induced biochemical defenses and N-regulated gene expression contribute to enhanced stress tolerance (Sun et al. 2020). The STRING-based predictions suggest that OsPR1 is co-expressed or functionally associated with enzymes involved in nitrogen and purine metabolism.

However, it is important to emphasize that these interactions are computational predictions based predominantly on co-expression, gene neighborhood and co-occurrence data, and have not yet been experimentally validated. Thus, the proposed link between OsPR1 and nitrogen metabolism should currently be considered a putative association.

Predicted secondary and 3D structures

Secondary structure analysis of OsPR1 using VADAR predicted that the protein consists of approximately 33% α-helix, 4% β-strand and 61% coil. These proportions are in line with previously reported CAP-domain proteins.

The 3D structure of OsPR1 was modeled using RoseTTAFold (Fig. 6A), and the AtPR1 structure was obtained from UniProt/AlphaFold (Fig. 6B). Ramachandran analysis of the OsPR1 model showed that 88% of residues fall within the most favored regions, 10% in additionally allowed regions, 1% in generously allowed regions and 1% in disallowed regions (Fig. 6C), indicating an overall reliable model.

Structural comparison using CLICK revealed a 57.14% structure overlap between OsPR1 and AtPR1 with an RMSD of 1.32 Å and a topology score of 0.93. Because topology scores range from 0 (completely dissimilar) to 1 (identical), these values support a high degree of 3D structural conservation between OsPR1 and AtPR1 (Nguyen et al. 2011). This finding is consistent with previous reports describing conserved structural features among PR proteins with enzymatic activity (Chu et al. 2022; dos Santos and Franco 2023).

Conclusions

In this study, we experimentally isolated and sequenced a rice PR1 gene, OsPR1, and performed an in-depth in silico characterization of the encoded protein. OsPR1 contains a conserved CAP domain and a signal peptide typical of secreted PR1 proteins. Phosphorylation site predictions suggest that OsPR1 may be regulated by protein kinases, while phylogenetic analysis places it within the monocot PR1 clade, closely related to PR1 proteins from *S. bicolor* and *Z. mays*. PPI network and KEGG pathway analyses suggest potential functional associations with nitrogen and purine metabolism, although these relationships remain to be experimentally validated. Structural modeling further indicates high 3D similarity between OsPR1 and AtPR1.

A deeper understanding of PR1 gene function in rice is important for elucidating stress-response networks and could, in the long term, support breeding strategies aimed at enhancing disease and stress tolerance. Future work should address OsPR1 expression patterns under biotic and abiotic stresses, subcellular localization, and targeted functional studies, including validation of predicted protein–protein interactions.

References

Akbudak MA, Yildiz S, Filiz E (2020) Pathogenesis related protein-1 (PR-1) genes in tomato (*Solanum lycopersicum* L.): Bioinformatics analyses and expression profiles in response to drought stress. Genomics 112(6):4089–4099.

Alexander D, Goodman RM, Gut-Rella M, Glascock C, Weymann K, Friedrich L, Maddox D, Ahl-Goy P, Luntz T, Ward E (1993) Increased tolerance to two oomycete pathogens in transgenic tobacco expressing pathogenesis-related protein 1a. PNAS 90(15):7327–7331.

Almeida-Silva F, Venancio TM (2022) Pathogenesis-related protein 1 (PR-1) genes in soybean: Genome-wide identification, structural analysis and expression profiling under multiple biotic and abiotic stresses. Gene 809:146013.

Anuradha C, Chandrasekar A, Backiyarani S, Thangavelu R, Giribabu P, Uma S (2022) Genome-wide analysis of pathogenesis-related protein 1 (PR-1) gene family from

Musa spp. and its role in defense response during stresses. Gene 821:146334.

Baek M, DiMaio F, Anishchenko I, Dauparas J, Ovchinnikov S, Lee GR, Wang J, Cong Q, Kinch LN, Schaeffer RD, et al. (2021) Accurate prediction of protein structures and interactions using a three-track neural network. Science 373(6557):871–876.

Breen S, Williams SJ, Outram M, Kobe B, Solomon PS (2017) Emerging insights into the functions of pathogenesis-related protein 1. Trends Plant Sci 22(10):871–879.

Chen N, Shao Q, Xiong Z (2023) Isolation and characterization of a pathogenesis-related protein 1 (SlPR1) gene with induced expression in tomato (*Solanum lycopersicum*) during *Ralstonia solanacearum* infection. Gene 855:147105.

Chu N, Zhou J-R, Rott PC, Li J, Fu H-Y, Huang M-T, Zhang H-L, Gao S-J (2022) ScPR1 plays a positive role in the regulation of resistance to diverse stresses in sugarcane (*Saccharum* spp.) and *Arabidopsis thaliana*. Ind Crops Prod 180:114736.

Cuadrado AF, Van Damme D (2024) Unlocking protein–protein interactions in plants: a comprehensive review of established and emerging techniques. J Exp Bot 75(17):5220–5236.

dos Santos C, Franco OL (2023) Pathogenesis-Related Proteins (PRs) with enzyme activity activating plant defense responses. Plants 12(11):2226.

Gasteiger E, Hoogland C, Gattiker A, Duvaud S, Wilkins MR, Appel RD, Bairoch A (2005) Protein identification and analysis tools on the ExPASy server. In Walker JM (Ed.). The Proteomics Protocols Handbook. Humana Press, Totowa, NJ, pp. 571–607.

Kattupalli D, Srinivasan A, Soniya EV (2021) A genome-wide analysis of pathogenesis-related protein-1 (*PR-1*) genes from *Piper nigrum* reveals its critical role during *Phytophthora capsici* infection. Genes (Basel) 12(7):1007.

Kumar S, Stecher G, Suleski M, Sanderford M, Sharma S, Tamura K (2024) MEGA12: Molecular Evolutionary Genetic Analysis Version 12 for adaptive and green computing. Mol Biol Evol 41(12):1-9.

Letunic I, Khedkar S, Bork P (2021) SMART: recent updates, new developments and status in 2020. Nucleic Acids Res 49(D1):D458-D460.

Liu Q, Xue Q (2006) Computational identification of novel *PR-1*-type genes in *Oryza sativa*. J Genet 85:193-198.

Nguyen MN, Tan KP, Madhusudhan MS (2011) CLICK—topology-independent comparison of biomolecular 3D structures. Nucleic Acids Res. 39(S2):W24-W28.

Sessa G, Yang X-Q, Raz V, Eyal Y, Fluhr R (1995) Dark induction and subcellular localization of the pathogenesis-related PRB-1b protein. Plant Mol Biol. 28(3):537–547.

Sun Y, Wang M, Mur LAJ, Shen Q, Guo S (2020) Unravelling the roles of nitrogen nutrition in plant disease defences. Int J Mol Sci 21(2):572.

Szklarczyk D, Kirsch R, Koutrouli M, Nastou K, Mehryary F, Hachilif R, Gable AL, Fang T, Doncheva NT, Pyysalo S, et al. (2023) The STRING database in 2023: protein–protein association networks and functional enrichment analyses for any sequenced genome of interest. Nucleic Acids Res. 51(D1):D638-D646.

van Loon LC, Rep M, Pieterse CMJ (2006) Significance of inducible defense-related proteins in infected plants. Annu Rev Phytopathol 44(1):135–162.

Wang J, Chitsaz F, Derbyshire MK, Gonzales NR, Gwadz M, Lu S, Marchler GH, Song JS, Thanki N, Yamashita RA, et al. (2023) The conserved domain database in 2023. Nucleic Acids Res 51(D1):D384-D388.

Willard L (2003) VADAR: a web server for quantitative evaluation of protein structure quality. Nucleic Acids Res 31(13):3316-3319.

Yao Q, Schulze WX, Xu D (2015) Phosphorylation site prediction in plants. Methods Mol Biol 1306:217-228.

Yin W, Bai Y, Wang S, Xu K, Liang J, Shang Q, Sa W, Wang L (2023) Genome-wide analysis of pathogenesis-related protein-1 (PR-1) genes from Qingke (*Hordeum vulgare* L. var. *nudum*) reveals their roles in stress responses. Heliyon 9(4):e14899.

Zaynab M, Peng J, Sharif Y, Al-Yahyai R, Jamil A, Hussain A, Khan KA, Alotaibi SS, Li S (2021) Expression profiling of pathogenesis-related Protein-1 (*PR-1*) genes from *Solanum tuberosum* reveals its critical role in phytophthora infestans infection. Microb Pathog 161:105290.